

Advanced flow noise reducing acoustic sensor arrays

Kevin Fine^a, Mark Drzymkowski^a, and Jay Cleckler^a
^aSARA, Inc., 6300 Gateway Drive, Cypress, CA, USA 90630

ABSTRACT

SARA, Inc. has developed microphone arrays that are as effective at reducing flow noise as foam windscreens and sufficiently rugged for tough battlefield environments. These flow noise reducing (FNR) sensors have a metal body and are flat and conformally mounted so they can be attached to the roofs of land vehicles and are resistant to scrapes from branches.

Flow noise at low Mach numbers is created by turbulent eddies moving with the fluid flow and inducing pressure variations on microphones. Our FNR sensors average the pressure over the diameter (~20 cm) of their apertures, reducing the noise created by all but the very largest eddies. This is in contrast to the acoustic wave which has negligible variation over the aperture at the frequencies of interest ($f \leq 400$ Hz).

We have also post-processed the signals to further reduce the flow noise. Two microphones separated along the flow direction exhibit highly correlated noise. The time shift of the correlation corresponds to the time for the eddies in the flow to travel between the microphones. We have created linear microphone arrays parallel to the flow and have reduced flow noise as much as 10 to 15 dB by subtracting time-shifted signals.

Keywords: flow noise, eddies, turbulence, acoustic sensors

1 INTRODUCTION

Flow noise limits the performance of unshielded microphone arrays at low frequencies. Figure 1 shows power density spectrums (PSD's) measured from a bare microphone mounted on the roof

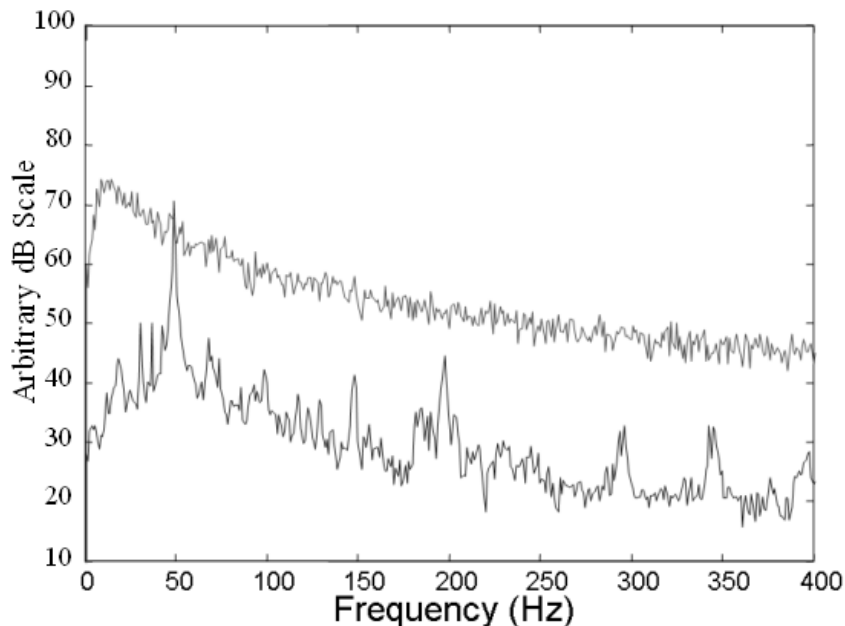


Figure 1: Microphone signals measured on top of a HMMWV. Upper curve: Microphone with no wind screen with vehicle moving at 24 km/hr. Lower curve: same microphone with vehicle at rest and engine at similar rpm.

of a HMMWV. The upper curve was measured at a speed of 24 km/hour, the lower curve with the vehicle at rest with the engine set to a similar rpm. The lower curve has several peaks from engine noise that are masked by the noise from the air flow over the microphone. Clearly flow noise must be removed in order to detect weak sources while a vehicle is moving, or even when it is at rest and there is wind.

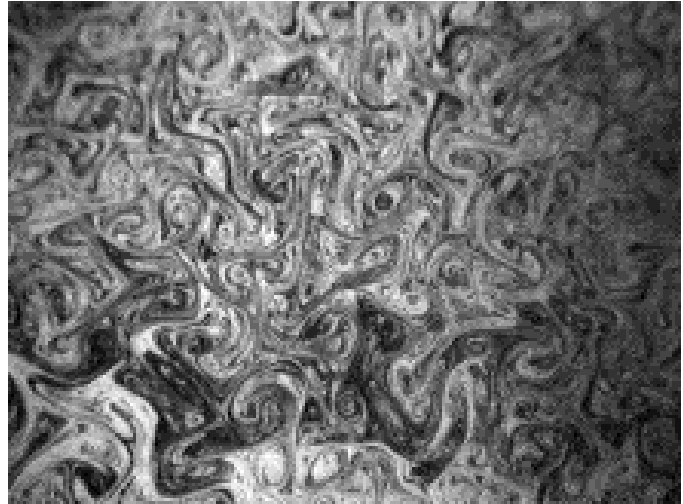


Figure 2: High Reynolds number turbulence.

Traditionally flow noise is removed with foam windscreens. While effective, they are not rugged enough for military conditions. Microphones need to be mounted on the outside of vehicles, where they are subjected to sand, water, snow and ice. They must survive severe vibrations and scrapes from branches and shrubs, and intense sunlight and temperature extremes.

At SARA we have developed flow noise reduction (FNR) sensors that replace microphones shielded with foam windscreens. These sensors come in rugged conformal packages that mount flush to vehicle roofs, allowing branches and shrubs to pass over without harm. They can survive harsh environmental conditions and are waterproof. And they match or exceed foam windscreens in removing flow noise.

In this paper we will describe the design and performance of these sensors. We will also discuss a limitation that remains with both these sensors and foam windscreens: flow noise at frequencies below 100 Hz. We will describe a current research project to decrease this low frequency noise by taking advantage of correlated properties of flow noise.

1.1 Low Mach number flow noise and turbulent eddies

Although acoustics is a result of fluid compressibility, low Mach number flow noise is caused by pressure fluctuations in an incompressible fluid,¹ which satisfies

$$\frac{\partial U_i}{\partial x_i} = 0, \quad (1)$$

where the U_i are the fluid velocity components and we use the summation convention. The incompressible Navier-Stokes equations are

$$\frac{\partial U_i}{\partial t} + U_j \frac{\partial U_i}{\partial x_j} = -\frac{1}{\rho} \frac{\partial p}{\partial x_i} + \nu \frac{\partial^2 U_i}{\partial x_j \partial x_j}, \quad (2)$$

where p is the pressure, ρ is the density, and ν is the kinematic viscosity. Taking the divergence and rearranging we have

$$\left[\frac{\partial}{\partial t} + U_j \frac{\partial}{\partial x_j} - \nu \frac{\partial^2}{\partial x_j \partial x_j} \right] \frac{\partial U_i}{\partial x_i} = -\frac{1}{\rho} \frac{\partial^2 p}{\partial x_i^2} - \frac{\partial U_i}{\partial x_j} \frac{\partial U_j}{\partial x_i}, \quad (3)$$

From Eq. 1, the left hand side is zero, so

$$\frac{\partial^2 p}{\partial x_i^2} = -\rho \frac{\partial U_i}{\partial x_j} \frac{\partial U_j}{\partial x_i}. \quad (4)$$

Thus we see that the velocity field is the source of pressure variations, since Eq. 4 is the Poisson equation with the source term coming from velocity derivatives.

For vehicle flow, the Reynolds number is large. Figure 2 is an image of turbulent flow at high Reynolds number. High Reynolds number turbulence is dominated by eddies, and the eddies are long-lasting since viscosity is small. Eq. 3 can be interpreted as the dynamic balance of eddies with a low or high pressure region in their centers which provide the centrifugal force to hold them together. In this regime turbulence can be approximated as eddies which are advected with the mean flow and slowly decay.² This model of flow noise is illustrated in Figure 3, which shows a microphone pair with eddies flowing by with velocity U . The acoustic signal $a(t)$ will be mixed with the pressure variations due these eddies, and this is the origin of low Mach number flow noise.

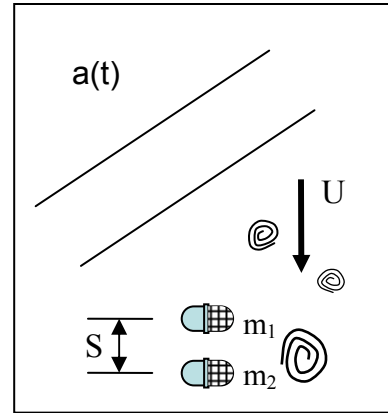


Figure 3: Vortices flowing past microphone pair along with acoustic wave.

2 Reducing flow noise with passive FNR sensors

In order to reduce flow noise, we need to create a structure that transmits pressure variations due to sound, but removes pressure variations due to eddies. One way to do this is to average the pressure variations over an aperture which is large compared to the eddies but small compared to the sound wavelengths. This is the principle used by our FNR sensors to remove flow noise.

Figure 4 depicts the concept. A microphone is placed inside a housing covered by a membrane. The structure is placed perpendicular to the flow, and eddies pass over the membrane, which averages the pressure variations from the eddies. While the eddies are coherent over their own extent, they are incoherent from one to another (ignoring effects like the Kalman vortex street), and only the smaller, averaged noise is transmitted to the microphone in the interior. This is in contrast to the acoustic wave, which at the frequencies of interest is constant over the membrane, and is transmitted unchanged into the interior. In addition, the housing and membrane provide an

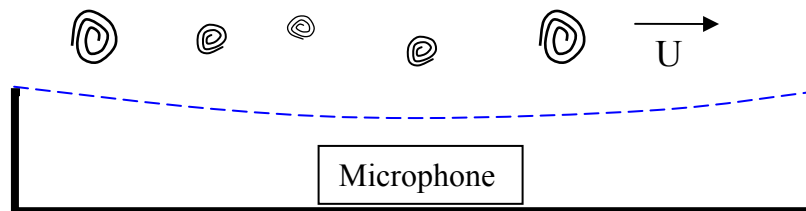


Figure 4: Conceptual drawing of FNR sensor.

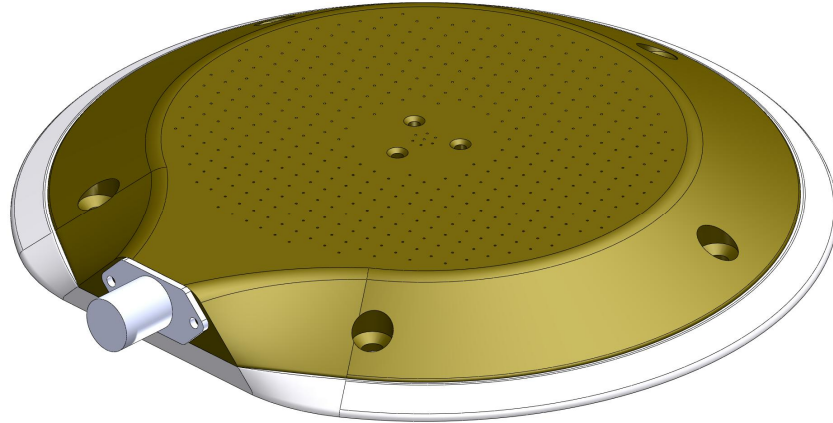


Figure 5: Conformal flow low noise reducing sensor package. Diameter is 6 inches. Noise reduction is nearly identical to foam ball, but package is much more rugged.

enclosure which protects the microphone from a harsh environment.

This is the general idea. It will probably not surprise the reader that it has taken years of careful work to evolve this idea into a practical sensor. We will only outline the general development path of our patent pending FNR sensors here.

The first improvement on Figure 4 is the addition of aerodynamic fairings to reduce inherent flow noise. The sharp edges on the housing would create eddies due to its interaction with the moving air, and the smooth fairing greatly reduces this source of noise. A second improvement is the use of vibration-reducing microphones. Due to the inertia of the elements, microphones are sensitive to vibrations, which are particularly severe in military environments. SARA has developed their own proprietary microphone arrangement to remove vibration noise.

The principle focus of our efforts has been the detailed design and choice of materials for the housing and membrane. We have tried various plastics and metals for the housing, and the same materials plus cloths for the membranes. We have found that most metals and plastics transmit the sound into the interior with small reduction in amplitude. A successful prototype was entirely constructed of aluminum, including the membrane, which did not include holes. While this arrangement provides good environmental protection and only small amplitude reduction, the effect on the relative phase of the acoustic signals versus frequency was troublesome. These phase differences can be removed using a calibration curve, but this consumes computing power, and the calibration curve varies between individual sensors.

In order to remove these phase variations, we have added small (~1 mm) holes to the membrane. We have also developed a model of the effect of the holes that has been useful in guiding the choice of placement and size of the holes. The result is a sensor that has very little amplitude and phase dependence. The disadvantage of the holes is that they allow water, dirt, and sand to enter into the chamber. The microphone and interior are waterproof, so water does not create a problem as long as it does not fill the chamber. Dirt and sand are more problematic, but our tests have shown that the holes are small enough that even fine sand particles take a long time to accumulate in the chamber. (for color images, please see electronic version of manuscript)

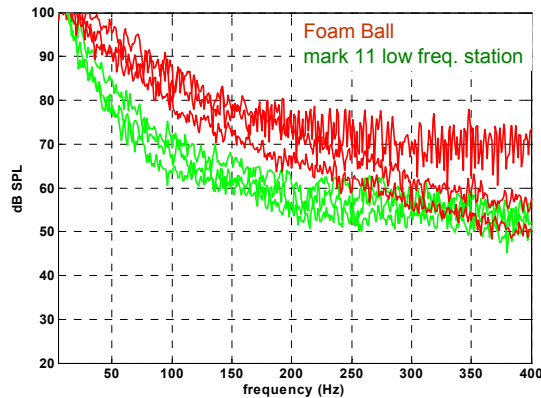


Figure 6: Flow noise comparison at 65 km/hr between foam ball (red) and SARA FNR sensor (green).

A recent single-element FNR design is shown in Figure 5. This unit is only 6 inches in diameter but still reduces noise about 20dB. It has optional underside or side-mounted connector configurations that are of military-grade for harsh environments. There is an optional base plate that allows for easy positioning on a vehicle and the small size gives the user space to customize array configurations. We have updated to a new microphone element capable of measuring a maximum sound level of 155dB SPL and an upper limit of 10 kHz in response. This unit is ideal for gun-shot detection. It also has high and low frequency channels that contain full signal conditioning/preamplifier circuitry embedded within the sensor.

Figure 6 shows a comparison between the power density spectra of flow noise on this sensor at 65 km/hr compared to a foam ball. It can be seen that the SARA FNR sensor outperforms the foam ball in reducing flow noise.

3 Reducing flow noise using correlation

The FNR sensors are effective at averaging over pressure variations created by eddies smaller than them. The situation is depicted in Figure 7, which shows large and small eddies with diameters L_L and L_S being advected by a flow with mean velocity U towards a sensor of diameter D . The eddies in the flow range in size from the size of the vehicle all the way down to the Kolmogorov dissipation scale, which is a few mm for air flow. These eddies have a three dimensional structure and consist of regions of both greater and smaller pressure than the mean. For eddies of diameters $L \ll D$ the pressure variations will be averaged away by the sensor and will create little noise on the signal. However, eddies with $L \gg D$ will not be averaged away. They will create noise at frequencies $f \ll U / D$, and the sensor is not effective in removing this low frequency flow noise. This noise can be seen at low frequency in Figure 6.

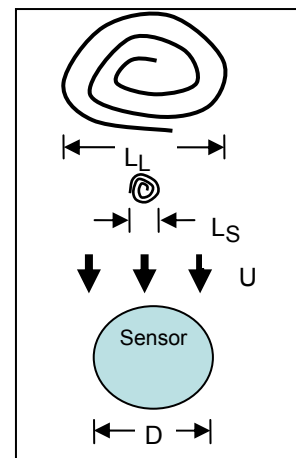


Figure 7: Eddies flow over an acoustic sensor.

We might take this argument to the extreme and try to remove low frequency noise by making a very large sensor. If D were the size of the vehicle roof, then all eddies would be averaged away

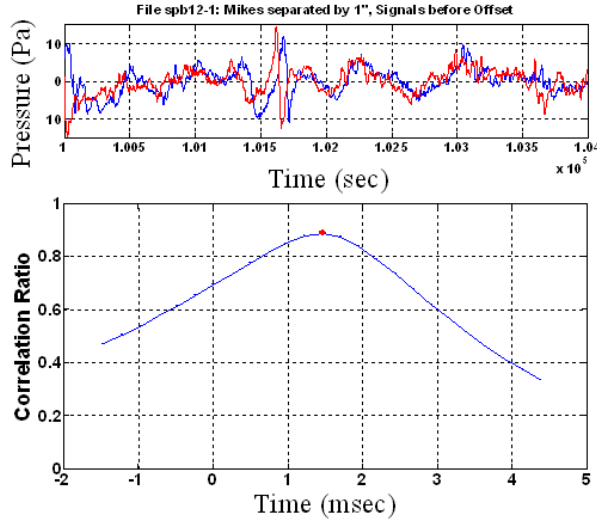


Figure 8: Measured signals on two microphones separated by 2.5 cm (top) and the correlation ratio between them (bottom).

and flow noise would disappear from the signal. However, besides being difficult to fit onto a crowded roof, very large sensors will also average away the acoustic signals that are the purpose of the sensor. Any sound wave with $f > U_S / D$, where U_S is the speed of sound, will also be reduced. Our typical FNR sensor has a D of about 10 cm, and can receive sound below 1.5 kHz.

3.1 The Role of Correlation in Flow Noise

Previous research has attempted to remove flow noise by using the correlation between hot-wire anemometer sensors and adjacent microphones.³ These anemometers are too delicate for battlefield applications, and we instead use the correlations between microphones separated in the downstream direction.⁴ Figure 8 is a measurement of flow noise on two adjacent microphones separated downstream by 2.5 cm in a 14 m/s airflow. Notice that one signal appears to be a time-delayed version of the other. This is confirmed by the peak in the correlation ratio between the two signals in the lower graph. Furthermore, this peak occurs at a time corresponding to the time it takes air to flow from one microphone to the other. This result would be expected from our model of flow noise coming from eddies creating pressure variations. Our strategy is to use this observation to subtract out flow noise from the signals.

3.2 Using Correlation to Remove Flow Noise

Figure 9 illustrates how correlated flow noise can be removed (it is a repeat of Figure 3). Two microphones m_1 and m_2 are separated by a distance S in the direction of a flow with mean velocity U . The flow carries eddies past the microphone and creates flow noise. Assuming that the eddies do not dissipate, and that they are the only source of noise, and that the flow noise is perfectly correlated we have

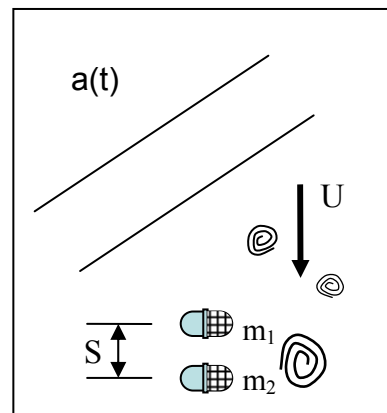


Figure 9: Vortices flowing past microphone pair along with acoustic wave.

$$\begin{aligned} m_1(t) &= a(t) + n(t) \\ m_2(t) &= a(t - \tau) + n(t - T), \end{aligned} \quad (5)$$

where $a(t)$ is the acoustic signal from a far away point source and $n(t)$ is the flow noise. The signals on microphone 2 include a time shift τ due to the angle of the acoustic source and the time $T=S/U$ for the flow to travel between the microphones. Defining

$$\delta(t) \equiv m_2(t) - m_1(t - T) = a(t - \tau) - a(t), \quad (6)$$

the flow noise has now been subtracted and has completely disappeared. However there are still two time-shifted copies of the sound signal. To disentangle them, we take the discrete Fourier transform of N points y_j defined by

$$Y_K = \sum_{j=1}^N y_j \exp\left\{\frac{(-2\pi i)(j-1)(k-1)}{N}\right\}. \quad (7)$$

(The sum starts at 1 instead of the usual 0 to follow the MATLAB convention.) Applying this transform to Eq. 6, we can extract the Fourier coefficients of $a(t)$:

$$A_K = \frac{\Delta_K}{\exp\left\{\frac{(-2\pi i)n_\tau(k-1)}{N}\right\} - \exp\left\{\frac{(-2\pi i)n_T(k-1)}{N}\right\}}, \quad (8)$$

where capital letters denote Fourier amplitudes, and n_τ and n_T are the offsets in number of points corresponding to τ and T . The A_K can be transformed back to the time domain, and we have a noise free acoustic signal.

We have extended this analysis for N microphones, with flow noise being removed by subtracting time shifted signals from each consecutive pair. The analysis is similar to above, except that the equations become matrices and N microphones can distinguish $N-1$ point sources.

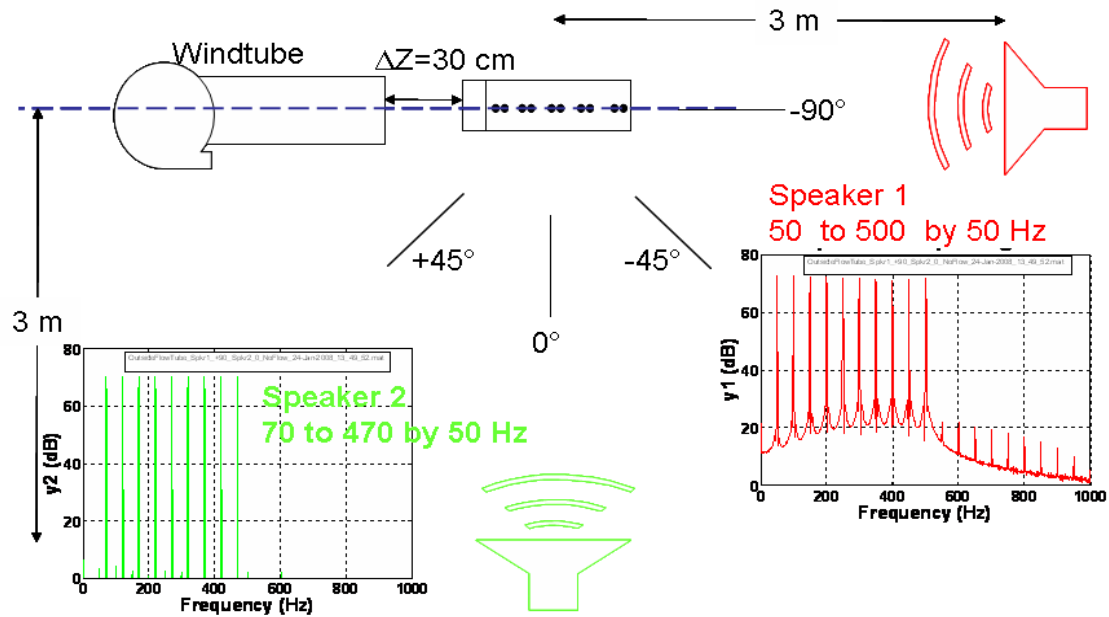


Figure 10: Schematic of experimental setup

3.3 Flow Tube Experiments

We performed measurements to test the above ideas using a flow tube. The flow tube consists of an electric motor driving a squirrel cage fan that drives air into a tube. The unit provides laminar air flow at a speed of about 14 m/s. The experiments were conducted outside, far from reflecting walls.

Figure 10 illustrates the experimental setup. As signal sources, we used portable, battery powered loudspeakers driven by compact disk players. There are two speakers; each located 3 meters distant from the microphone array, and broadcasting two different recorded sounds. Speaker 1 has tones at 50 to 500 Hz spaced at 50 Hz intervals; speaker 2 has 70 to 470 Hz spaced by 50 Hz intervals. These two sources are essentially two interleaved combs of frequencies.

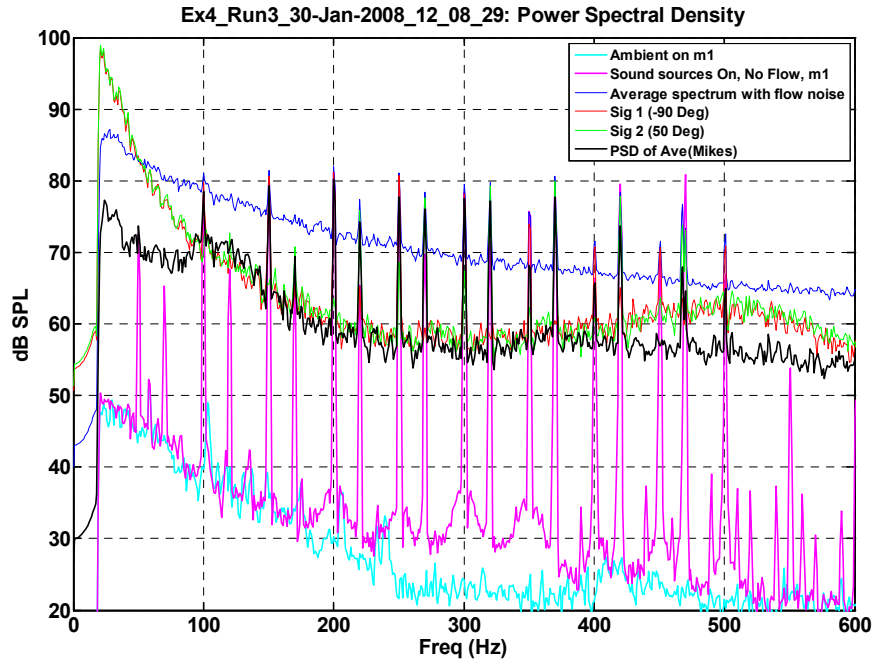


Figure 11: Power density spectra from data taken with speaker 1 at -90° and speaker 2 at $+90^\circ$.

The microphone array was placed 30 cm from the exit of the flow tube. The array consisted of ten microphones arranged as five pairs of two microphones spaced by approximately 2 cm. Figure 11 shows power density spectra of data taken with speaker 1 at -90° and speaker 2 at $+90^\circ$.

First an ambient is shown, which is the lowest (cyan) curve. This shows a $1/f$ type characteristic noise floor of ambient noise. Then, the two speakers were turned on, with no flow noise, resulting in the highly spiked spectrum shown just above the ambient (magenta curve). Each large peak alternates coming from speaker 1 and 2, with some smaller peaks coming from harmonic distortion in the speakers.

Next, the flow tube is turned on, adding flow noise to the system. The highest (blue) curve is calculated by taking the PSD's of each raw microphone signal and averaging them together. This peak shows a 40 to 50 dB increase in broadband levels due to the presence of flow noise. Speaker tones that are large enough can be identified in this averaged signal.

Next our flow noise algorithm was applied to the microphone signals to extract the red and green curves (the curves below the average microphone signal which have a hump near 500 Hz). These curves show a reduction of broad band noise of more than 10 dB for some frequencies. It is interesting to compare them to a signal formed by just averaging the ten microphone signals together and then taking the PSD (black curve). This curve is very similar to the extracted signals, except it does not show the curious hump at 500 Hz and the divergence at low frequencies. These will be explained in the next section.

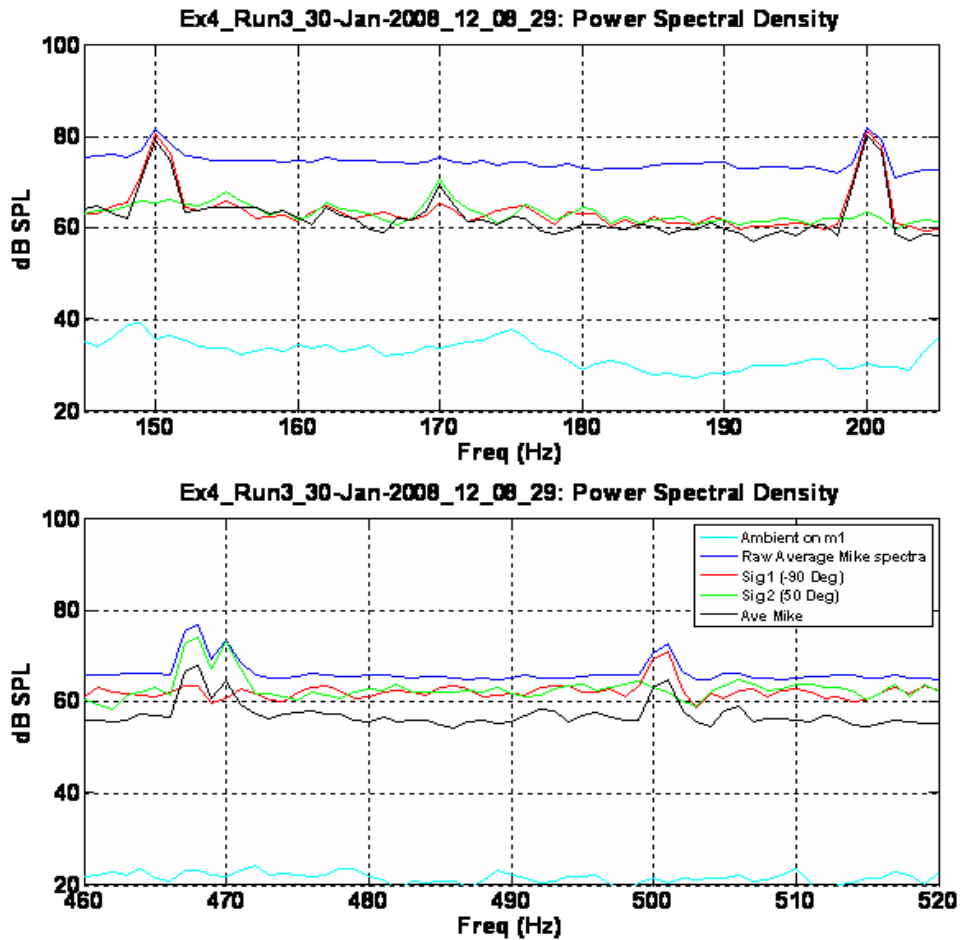


Figure 12: Magnification of spectra near 175 Hz and 490 Hz. Same data as previous figure.

Figure 12 is a magnification of the previous figure around 175 and 490 Hz. It can be seen that the algorithm separates the peaks between the sources unlike the average signal (in black) which shows all peaks. The peaks are smaller in the average signal at the higher frequency due to partial cancellation between the microphones.

It would be interesting to compare the performance of this algorithm to a beam forming algorithm, but we have not yet done this. Theoretically, beam forming relies upon averaging incoherent noise to improve signal to noise, and would work less well with coherent noise.

3.4 Applying the algorithm to reducing noise in FNR sensors

The measurements in this experiment were not taken with FNR sensors, and contain large flow noise across the frequency spectrum. We now consider the question of using this algorithm with FNR sensors, where the only flow noise remaining is at low frequencies. At first sight this seems unpromising, due to the “infra-red” divergence of the algorithm at low frequencies.

There is an intuitive explanation for this infra-red divergence. At low frequencies, we are subtracting signals with very small phase differences, and it is necessary to multiply the difference by a large factor to recover the sound. The large factor also multiplies the uncorrelated noise, which is not small when the two signals are subtracted. Therefore the uncorrelated noise becomes very large, resulting in poor signal to noise ratio. This logic also explains the curious hump near 500 Hz, since at this frequency we phase shift one signal by about 2π relative to the other, which requires a similar large factor multiplying the sound.

This explanation implies that the frequency below which the divergence begins scales as $U / \Delta L$, where ΔL is the spacing between microphones and U is the flow velocity. In order to push this flow noise to lower frequencies we need to use microphone pairs with larger spacing. However, at longer distances the correlation of the flow noise decreases, and subtraction is less effective at eliminating noise.

This is less likely to be true for the signals from FNR sensors, since the high frequency flow noise has already been removed and lower frequency flow noise has longer correlation length. It remains to be seen if this algorithm can reduce low frequency flow noise with FNR sensors; however, very modest reductions in noise can significantly increase the range of low frequency target detection.

4 Conclusion

SARA has developed flow noise reducing sensors that are rugged enough for use on the top of military vehicles. They are as effective at removing flow noise as foam balls. Both foam balls and our FNR sensors are less successful at removing very low frequency ($f \leq 100$ Hz) flow noise which is a critical range for detecting some military targets. Currently we are developing an algorithm based upon subtracting correlated noise to improve the performance for this range.

5 Acknowledgements

The authors would like to thank Jay Chang, Lisa Thier, and Anthony Rotolo at the Army Acoustic Center of Excellence (ARDEC) for their current support, and we would also like to thank Tien Pham, Raju Demarla, and Dale Robertson at the Army Research Laboratories for their continued support.

References

¹A clear overview of flow noise can be found in Morgan, “*An Investigation of the Sources and Attenuation of Wind Noise in Measurement Microphones*,” Doctoral Thesis, University of Mississippi, 1993.

²Wilson, DK, et. al. “Spatial structure of low-frequency wind noise,” *J. Acoust. Soc. Am.*, Vol. **122**, No. 6, December, 2007.

³McGuinn, RS, et. al. “*Low Flow-Noise Microphone for Active Noise Control Applications*,” *AIAA Journal*, Vol. **25**, No. 1, Jan, 1997.

⁴Shields, FD. “*Low-frequency wind noise correlation in microphone arrays*,” *J. Acoust. Soc. Am.*, Vol. **117**, No. 6, June, 2005.